Available online at www.sciencedirect.com
ScienceDirect
Quaternary Research 69 (2008) 42–55
QUATERNARY RESEARCH
www.elsevier.com/locate/yqres

Using cryptotephras to extend regional tephrochronologies: An example from southeast Alaska and implications for hazard assessment

Richard Payne [a,b,c,*], Jeffrey Blackford [c], Johannes van der Plicht [d,e]

[a] Department of Geography, Queen Mary, University of London, Mile End Road, London, E1 4NS, UK
[b] Department of Biology, University of Bergen, Allègaten 41, N-5007 Bergen, Norway
[c] Geography, School of Environment and Development, The University of Manchester, Oxford Road, Manchester, M13 9PL, UK
[d] Centre for Isotope Research, University of Groningen, P.O. Box 72, 9700 AB Groningen, The Netherlands
[e] Faculty of Archaeology, Leiden University, The Netherlands

Received 12 March 2007
Available online 11 December 2007

Abstract

Cryptotephrochronology, the use of hidden, diminutive volcanic ash layers to date sediments, has rarely been applied outside western Europe but has the potential to improve the tephrochronology of other regions of the world. Here we present the first comprehensive cryptotephra study in Alaska. Cores were extracted from five peatland sites, with cryptotephras located by ashing and microscopy and their glass geochemistry examined using electron probe microanalysis. Glass geochemical data from nine tephras were compared between sites and with data from previous Alaskan tephra studies. One tephra present in all the cores is believed to represent a previously unidentified eruption of Mt. Churchill and is named here as the 'Lena tephra'. A mid-Holocene tephra in one site is very similar to Aniakchak tephra and most likely represents a previously unidentified Aniakchak eruption, ca. 5300–5030 cal yr BP. Other tephras are from the late Holocene White River eruption, a mid-Holocene Mt. Churchill eruption, and possibly eruptions of Redoubt and Augustine volcanoes. These results show the potential of cryptotephras to expand the geographic limits of tephrochronology and demonstrate that Mt. Churchill has been more active in the Holocene than previously appreciated. This finding may necessitate reassessment of volcanic hazards in the region.

Keywords: Tephra; Cryptotephra; Radiocarbon; White River Ash; Mt. Churchill; Aniakchak; Alaska; Holocene

Introduction

Explosive volcanic eruptions typically produce large amounts of volcanic ash (tephra), which may be deposited across a wide area. Layers of tephra preserved in peat, lake, and marine sediments provide a means of correlating sequences and, when the tephra can be identified to an eruption of known age, a method of dating sediments. Traditional tephrochronology has concentrated on tephra layers that are visible to the naked eye. These visible tephra layers are only present relatively near to the source volcanoes and limit the potential of tephrochronology. More recently, non-visible tephras have been identified that can only be detected by microscopy (termed cryptotephras or microtephras; Lowe and Hunt, 2001). Using cryptotephras, the limits of Icelandic tephra deposition have been expanded to cover much of northwest Europe. To date, Icelandic tephras have been identified in Ireland, England, Wales, Scotland, Norway, Sweden, Germany, Greenland, the Netherlands, and the Faroe Islands (Persson, 1971; Mangerud et al., 1984; Dugmore, 1989; Merkt et al., 1993; Pilcher et al., 1995; Pilcher and Hall, 1996; Birks et al., 1996; Gronvold et al., 1995; Wastegård et al., 2001; Hall and Pilcher, 2002; Buckley and Walker, 2002; Bergman et al., 2004; Davies et al., 2005). More than 12 Holocene tephra isochrons have been identified (Dugmore et al., 1995; Van den Bogaard and Schmincke, 2002).

With only a few exceptions (Zoltai, 1988; Gehrels et al., 2006), cryptotephrochronology has not been applied outside western Europe. Cryptotephra studies have several advantages over conventional approaches. Cryptotephrochronology allows

* Corresponding author. Geography, School of Environment and Development, The University of Manchester, Oxford Road, Manchester, M13 9PL, UK.
E-mail address: Richard.Payne-2@manchester.ac.uk (R. Payne).

0033-5894/$ - see front matter © 2007 University of Washington. All rights reserved.
doi:10.1016/j.yqres.2007.10.007

tephras to be identified in sites farther from the volcanic sources where no visible tephras are present, increasing the geographic potential for tephrochronology. In sites where visible tephras are present, cryptotephrochronology may increase the tally of tephra isochrons and thereby expand the dating framework. Cryptotephra studies may allow detection of previously unidentified eruptions where proximal deposits are poorly preserved or masked by subsequent eruptions. Even diminutive cryptotephras may be associated with environmental impacts (Blackford et al., 1992; Dwyer and Mitchell, 1997); cryptotephra studies are therefore necessary to understand the spatial extent of volcanic impacts on the environment. These advantages are equally applicable to other volcanic regions where only visible tephras have been studied to date.

Alaska contains over 100 Quaternary volcanoes, approximately 8% of the Earth's active, above-water volcanoes. Alaskan volcanoes have had several thousand Holocene eruptions and visible tephra layers are found over a large portion of the state, with the greatest concentrations in the south and west. The southeast Alaskan panhandle is distant from the majority of Alaskan volcanoes and has virtually no Holocene tephrostratigraphy. There is only one volcano in the region, Mt. Edgecumbe on Kruzof Island, near Sitka. Tephra from a Younger Dryas-age Edgecumbe eruption (ca. 11,250 ^{14}C yr BP) is found in many sites in the region (McKenzie, 1970; Riehle et al., 1992; Begét and Motyka, 1998). In the Holocene, it is believed that the volcano had two more minor eruptions around 4000–6000 ^{14}C yr BP, but tephra from these events is only found closely adjacent to the volcano (Riehle and Brew, 1984; Riehle, 1996). North of the region is the Wrangell Volcanic Field, a group of Quaternary volcanoes that have had several Holocene eruptions. The best known product of these eruptions is twin tephra layers, collectively termed the 'White River Ash' (WRA), representing two large volcanic eruptions around 1200 and 1900 cal yr BP. WRA tephra is dispersed across approximately 540,000 km^2 of eastern Alaska, Yukon, and the Northwest Territories but is not known as far south as the sites studied here (Robinson, 2001; Lerbekmo and Campbell, 1969).

Southeast Alaska also contains numerous peatlands. Peatlands are an excellent medium for tephrostratigraphy. The moist, vegetated surfaces of mires are effective at trapping tephra particles. Some tephra particles may move several centimeters down through the peat, but the majority appear to remain trapped at the surface, forming a defined layer that accurately records the position of the mire surface at the time of eruption (Dugmore and Newton, 1992; Payne et al., 2005; Gehrels et al., 2006). Most tephra particles preserved in peat undergo limited geochemical change over millennia, although exceptions may exist for some tephras and in some peat environments (Hodder et al., 1991; Dugmore et al., 1992; Pollard et al., 2003). Extracting glass shards from peat is simple compared to other sediments using a straightforward acid-digestion method (Persson, 1971; Dugmore, 1989; Rose et al., 1996). Although recent studies have demonstrated that high-resolution cryptotephrochronologies can be produced from lake sediments, the majority of studies to date have used peatlands (Chambers et al., 2004). It is tephra layers in peatlands that have provided the basis of the Holocene cryptotephrochronology of Europe.

Southeast Alaska is a highly suitable location to demonstrate the value of cryptotephrochronology. Although the area has essentially no recognized Holocene tephrostratigraphy, the European cryptotephra record suggests that it is close enough to volcanic sources for cryptotephras to be present. Visible WRA deposits are found within 100 km of the sites considered

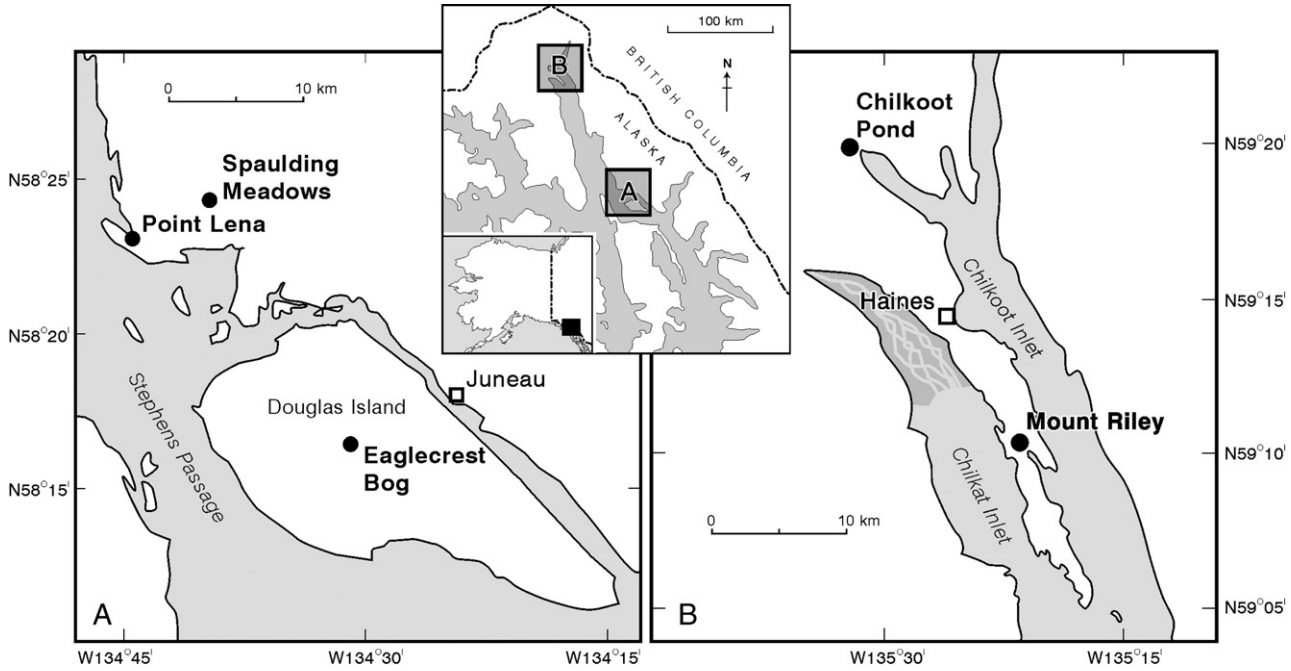

Figure 1. Location map of peatland sites used in this study.

https://doi.org/10.1016/j.yqres.2007.10.007 Published online by Cambridge University Press

here, and prevailing wind directions may serve to direct tephra from more distant eruptions towards the region. The area also has numerous peatland sites suitable for tephrochronology and is the site of ongoing palaeoenvironmental research for which tephras may provide a dating framework. Given this setting, the aims of this study are therefore

1. to establish the outline of Holocene tephrochronology for the region;
2. to provide age estimates for any tephra layers recovered; and
3. to add to our knowledge of the eruptive history of volcanoes in the wider region, recognizing any implications for volcanic hazard assessment.

Methods

Five peatland sites were investigated. The sites are *Sphagnum*-dominated oligotrophic peatlands and encompass a range of mire types present in the region including raised bog (Point Lena), upland blanket mires (Mount Riley, Spaulding Meadows), an intermediate site (Eaglecrest Bog), and a minerotrophic lake-margin peatland (Chilkoot Pond) (Rigg, 1914, 1937; Dachnowski-Stokes, 1941; Payne and Blackford, 2004) (Fig. 1).

Cores were extracted from the deepest areas of peat using a 50-mm-bore Russian pattern corer, with monolith blocks (approximately 100 × 100 × 300 mm) cut from the surface where the peat was not solid enough to allow coring (Aaby and Digerfeldt, 1986). Extracted cores were placed in gutter tubing, wrapped in plastic, and returned to the laboratory. Cryptotephra layers were identified by ashing and microscopy (Pilcher and Hall, 1992). Contiguous 50-mm-long samples were removed, dried, and incinerated at 550°C for 10 h. Samples were weighed pre- and post-burning and these data used to calculate loss on ignition (LOI), which can provide an aid to identifying the thickest layers. The residue remaining after incineration was washed in 10% HCl and distilled water and centrifuged at 3000 RPM to concentrate shards. A *Lycopodium* spore inoculum was added to allow a quantitative count of glass shards (Stockmarr, 1971; Caseldine et al., 1998). Slides were prepared by mixing a drop of the prepared sample with a drop of glycerol on a clean microscope slide. Tephra slides were examined microscopically at 400× magnification, and glass shards were identified by their distinctive morphology, vesicularity, and colour. Where significant numbers of glass shards were identified, the core was subsampled at 10-mm resolution and the preparation was repeated as above to locate the region of maximum glass concentration and to produce a concentration profile.

The ashing methodology allows rapid and straightforward tephra preparations but is unsuitable for geochemical studies because of the possibility for geochemical changes during heating. Samples for electron probe microanalysis (EPMA) were prepared from all major tephra zones using acid digestion (Persson, 1971; Dugmore, 1989). A 1- to 2-cm^3 peat sample was added to 50 ml of concentrated sulphuric acid. Several milliliters of concentrated nitric acid were gradually added and the solution was heated to remove all organic material. The acid solution was diluted with distilled water and the sample centrifuged to concentrate shards. This dilution process was repeated until the pH of the solution was near neutral. Thin sections for EPMA were prepared by evaporating the solution on a heated slide and mixing the tephra with an epoxy resin. The resin layer was ground down using successively finer grit-papers and polished using 6-μm and 1-μm diamond pastes before being carbon coated. The acid digestion methodology has been used in most cryptotephra studies to date. However, it has recently been suggested that acid treatments may lead to cation leaching (Blockley et al., 2005). The effects of leaching on EPMA data are likely to be minimized by sample polishing and it is unlikely to have significantly affected the results reported here.

The glass shard major element compositions were assayed using wavelength-dispersive EPMA, the standard geochemical technique used in most tephra studies. Two machines were used, each with slightly different operating conditions. Both machines were calibrated using a sequence of minerals and metals of known composition and an andradite standard analysed at frequent intervals to identify any instrumental drift. Samples with a 'B' notation were analysed using the ARL-SEMQ microprobe at the Department of Earth Science, University of Bergen. Operating conditions were a 15-kV accelerating voltage, a 10-nA beam current, and a 1-μm beam. Samples with an 'E' notation were analysed on the Cameca SX100 microprobe at the School of Geosciences, University of Edinburgh, using a 20-kV accelerating voltage and a 4-nA beam current. Where shard size permitted, the beam was rastered over a 10 × 10 μm grid to minimize sodium and potassium loss, although for some samples this was not possible and in these a static 1-μm beam was used. The choice of microprobe was dictated by practical considerations and does not relate to any intrinsic differences between the two sets of samples.

To examine the correlation between tephras found in this study and with those previously examined, a variety of techniques were investigated. Bi-plots and ternary diagrams were constructed for selected major oxides. Correlations within the data set and with the previous studies were tested using similarity coefficients (Borchardt et al., 1972), a technique for comparing average percentages of major oxides of glasses between tephra pairs. The similarity coefficient (SC) is calculated as the averaged ratio of normalized oxides using the lesser value as the numerator. Following Riehle (1985), oxides with a maximum value of less than 0.4% are excluded from the calculation. SCs greater than or equal to 0.95 have been considered to show close correlation, while SCs of 0.90–0.94 may indicate a different tephra from the same source. An SC less than 0.90 indicates no correlation (Borchardt et al., 1972; Riehle, 1985; Begét et al., 1992), although these general rules need to be treated with caution. SC matrices were constructed to compare tephras within our data set and with a large data set compiled from previously published tephra analyses in southern Alaska (Riehle, 1985; Riehle et al., 1987; Riehle and Bowers, 1990; Riehle et al., 1992, 1999 (selected data); Downes, 1985; Begét et al., 1991; 1992; Richter et al., 1995; Begét and Motyka, 1998; Child et al., 1998). The SC technique has the advantages of being

https://doi.org/10.1016/j.yqres.2007.10.007 Published online by Cambridge University Press

Table 1
EPMA data for southeast Alaskan tephras

SPM 26

	B	B	B	B	B	B	Mean	Mean norm.	σ
SiO_2	72.43	72.69	73.14	71.66	72.81	70.89	72.27	75.87	1.01
TiO_2	0.23	0.19	0.14	0.12	0.18	0.14	0.17	0.17	0.04
Al_2O_3	14.14	14.29	13.03	13.17	12.83	13.20	13.44	14.11	0.51
FeO	1.44	1.44	1.02	1.17	1.01	1.40	1.25	1.31	0.21
MnO	0.05	0.07	0.04	0.01	0.10	0.00	0.05	0.05	0.04
MgO	0.31	0.43	0.16	0.19	0.14	0.32	0.26	0.27	0.12
CaO	1.86	1.85	1.43	1.48	1.40	1.77	1.63	1.71	0.22
Na_2O	3.92	1.94	3.61	3.13	2.32	3.26	3.03	3.18	0.78
K_2O	3.14	2.96	3.26	3.39	3.35	2.98	3.18	3.34	0.21
	97.51	95.85	95.82	94.31	94.14	93.96	95.27		

ECR 32

	B	B	B	B	B	B	B	B	B	B	B	B	Mean	Mean norm.	σ
SiO_2	73.17	71.19	71.68	71.92	72.72	71.42	72.12	71.40	72.38	72.98	70.08	70.54	71.80	75.30	0.93
TiO_2	0.25	0.15	0.23	0.21	0.18	0.24	0.18	0.16	0.05	0.14	0.18	0.17	0.18	0.19	0.05
Al_2O_3	14.23	14.19	13.96	13.55	12.94	13.93	14.07	13.17	12.71	12.97	13.71	13.30	13.56	14.22	0.48
FeO	1.52	1.50	1.49	1.45	0.97	1.48	1.40	1.07	0.88	0.96	1.34	1.40	1.29	1.35	0.25
MnO	0.13	0.00	0.00	0.00	0.09	0.06	0.08	0.00	0.06	0.04	0.10	0.02	0.05	0.05	0.05
MgO	0.39	0.35	0.37	0.36	0.23	0.38	0.38	0.19	0.18	0.12	0.28	0.29	0.29	0.31	0.09
CaO	1.89	1.88	1.87	1.83	1.37	1.77	1.76	1.43	1.35	1.40	1.71	1.79	1.67	1.75	0.22
Na_2O	3.47	3.78	3.56	3.55	3.73	3.09	2.11	3.86	3.56	2.39	3.55	3.57	3.35	3.51	0.58
K_2O	3.10	3.02	3.00	3.03	3.54	3.06	3.15	3.41	3.37	3.41	3.08	2.90	3.17	3.33	0.22
	98.14	96.06	96.15	95.89	95.76	95.41	95.25	94.68	94.55	94.41	94.04	93.99	95.36		

LNA 39

	B	B	B	B	E	E	E	E	E	E	E	E	Mean	Mean norm.	σ
SiO_2	73.31	71.27	70.64	70.56	73.17	73.41	69.86	71.45	71.49	70.98	70.53	70.96	71.47	74.87	0.63
TiO_2	0.19	0.16	0.19	0.18	0.25	0.17	0.16	0.00	0.12	0.24	0.11	0.20	0.16	0.17	0.07
Al_2O_3	14.34	13.69	14.00	13.27	14.09	13.12	13.67	13.43	13.56	13.25	13.59	13.08	13.59	14.24	0.32
FeO	1.42	1.40	1.49	1.41	1.67	0.94	1.35	1.46	1.45	1.45	1.52	1.49	1.42	1.49	0.18
MnO	0.06	0.07	0.04	0.06	0.00	0.12	0.06	0.01	0.03	0.08	0.06	0.01	0.05	0.05	0.03
MgO	0.34	0.39	0.36	0.35	0.39	0.19	0.47	0.39	0.35	0.41	0.43	0.42	0.37	0.39	0.08
CaO	1.81	1.79	1.83	1.56	1.94	1.31	1.86	1.98	1.72	1.83	1.71	1.73	1.75	1.84	0.19
Na_2O	3.85	3.64	3.79	3.60	2.73	4.12	4.41	3.03	3.01	3.33	3.31	3.13	3.50	3.66	0.51
K_2O	3.25	3.03	2.93	3.22	3.07	3.45	3.14	3.10	2.99	3.04	3.12	3.27	3.13	3.28	0.14
	98.56	95.44	95.27	94.20	97.30	96.82	94.99	94.84	94.72	94.60	94.37	94.29	95.45		

(continued on next page)

Table 1 (*continued*)

LNA 100

	B	B	B	B	B	B	B	B	B	B	B	B	Mean	Mean norm.	σ
SiO_2	73.23	72.05	72.22	71.83	72.12	70.46	72.45	70.53	71.56	70.86	72.44	70.30	71.67	74.48	0.83
TiO_2	0.20	0.28	0.24	0.14	0.23	0.23	0.09	0.31	0.14	0.18	0.10	0.14	0.19	0.20	0.07
Al_2O_3	14.39	14.38	14.30	14.10	14.34	14.58	13.31	13.66	13.72	14.07	13.00	13.68	13.96	14.51	0.42
FeO	1.51	1.56	1.48	1.46	1.58	1.37	1.14	1.71	1.35	1.47	0.96	1.44	1.42	1.47	0.20
MnO	0.02	0.09	0.10	0.04	0.10	0.05	0.01	0.11	0.04	0.00	0.01	0.00	0.05	0.05	0.04
MgO	0.31	0.28	0.36	0.35	0.32	0.30	0.31	0.77	0.24	0.39	0.19	0.32	0.35	0.36	0.15
CaO	1.89	1.94	1.90	1.89	1.89	2.15	1.49	2.12	1.76	1.87	1.31	1.89	1.84	1.91	0.24
Na_2O	3.63	3.89	3.80	3.59	2.70	4.01	3.76	3.76	3.60	3.88	3.53	3.65	3.65	3.79	0.34
K_2O	3.20	3.00	3.00	3.10	3.09	2.95	3.43	2.90	3.32	2.99	3.34	2.90	3.10	3.22	0.19
	98.38	97.49	97.39	96.49	96.37	96.10	95.99	95.89	95.73	95.71	94.87	94.30	96.22		

MTR 190

	B	E	Mean	Mean norm.	σ
SiO_2	77.30	73.27	75.28	77.61	2.22
TiO_2	0.12	0.11	0.11	0.12	0.01
Al_2O_3	11.73	13.28	12.50	12.90	1.25
FeO	1.00	1.13	1.07	1.10	0.11
MnO	0.03	0.09	0.06	0.06	0.04
MgO	0.13	0.29	0.21	0.21	0.12
CaO	0.76	1.31	1.03	1.07	0.42
Na_2O	3.52	3.51	3.52	3.63	0.03
K_2O	3.05	3.36	3.21	3.31	0.26
	97.63	96.36	97.00		

CHP 184

	B	B	B	B	B	B	B	B	B	B	B	B	Mean	Mean norm.	σ
SiO_2	73.39	74.58	74.77	74.79	74.81	72.52	74.63	73.55	73.57	71.98	72.48	72.88	73.66	75.64	0.87
TiO_2	0.17	0.12	0.11	0.11	0.20	0.23	0.13	0.15	0.16	0.14	0.12	0.08	0.14	0.15	0.04
Al_2O_3	14.57	13.75	13.63	13.57	13.41	14.14	13.63	13.62	13.42	14.16	13.34	12.80	13.67	14.04	0.39
FeO	1.55	1.14	1.07	1.04	1.06	1.48	1.12	1.13	1.12	1.41	1.12	0.97	1.18	1.21	0.19
MnO	0.02	0.05	0.01	0.02	0.05	0.09	0.11	0.03	0.00	0.05	0.11	0.09	0.05	0.05	0.04
MgO	0.41	0.28	0.19	0.22	0.23	0.36	0.16	0.22	0.15	0.31	0.24	0.10	0.24	0.24	0.09
CaO	1.90	1.46	1.46	1.46	1.40	1.87	1.48	1.51	1.56	1.78	1.48	1.31	1.56	1.60	0.19
Na_2O	3.87	3.90	3.81	3.80	3.45	3.58	2.68	3.62	3.56	3.51	3.41	3.19	3.53	3.62	0.32
K_2O	3.09	3.45	3.44	3.40	3.51	3.11	3.41	3.44	3.24	3.37	3.40	3.41	3.36	3.45	0.15
	98.98	98.72	98.50	98.41	98.13	97.37	97.34	97.26	96.78	96.71	95.68	94.82	97.39		

ECR 100

	E	E	Mean	Mean norm.	σ
SiO_2	75.08	74.92	75.00	78.77	0.50
TiO_2	0.32	0.46	0.39	0.41	0.10
Al_2O_3	11.28	10.90	11.09	11.65	0.19
FeO	1.30	1.57	1.44	1.51	0.21
MnO	0.07	0.05	0.06	0.06	0.01
MgO	0.28	0.20	0.24	0.25	0.06
CaO	1.68	1.43	1.55	1.63	0.18
Na_2O	3.92	3.15	3.53	3.71	0.55
K_2O	1.81	2.02	1.91	2.01	0.17
	95.74	94.69	95.21		

ECR 162

	E	E	E	E	E	E	E	E	E	E	E	E	E	E	E	E	E	E	E	E	Mean	Mean norm.	σ
SiO_2	71.49	70.15	69.89	70.50	70.30	69.50	69.63	70.14	69.23	68.67	69.12	69.56	69.28	69.10	68.88	68.55	69.44	68.65	68.26	67.96	67.90	69.34	72.33	0.38
TiO_2	0.46	0.39	0.56	0.54	0.33	0.48	0.48	0.44	0.58	0.59	0.49	0.44	0.40	0.56	0.50	0.50	0.45	0.58	0.62	0.52	0.55	0.50	0.52	0.08
Al_2O_3	14.81	14.57	14.60	14.73	14.54	14.37	14.31	14.17	14.41	13.96	14.30	13.87	14.24	14.15	13.86	14.09	13.94	14.27	14.21	14.19	14.10	14.27	14.88	0.17
FeO	2.25	2.30	2.40	2.46	2.47	2.49	2.43	2.45	2.44	2.33	2.40	2.41	2.41	2.38	2.46	2.33	2.27	2.37	2.39	2.56	2.37	2.40	2.50	0.09
MnO	0.16	0.24	0.15	0.14	0.17	0.22	0.15	0.11	0.15	0.18	0.14	0.17	0.10	0.18	0.16	0.19	0.16	0.13	0.17	0.14	0.16	0.16	0.17	0.03
MgO	0.52	0.53	0.49	0.54	0.52	0.48	0.53	0.45	0.48	0.61	0.49	0.47	0.48	0.47	0.54	0.50	0.48	0.50	0.51	0.54	0.54	0.51	0.53	0.04
CaO	1.84	1.70	1.73	1.65	1.72	1.84	1.69	1.61	1.67	1.50	1.67	1.72	1.56	1.58	1.77	1.68	1.75	1.80	1.61	1.55	1.81	1.69	1.76	0.10
Na_2O	4.18	4.69	4.36	3.72	4.05	4.21	3.78	3.68	3.86	4.76	3.88	3.87	3.96	3.90	3.99	4.20	3.61	3.70	4.04	3.91	3.68	4.00	4.17	0.31
K_2O	3.09	3.21	3.12	2.99	3.10	2.85	3.05	2.91	3.03	3.12	3.07	2.98	2.91	2.98	3.01	3.05	2.92	2.94	2.88	3.08	2.99	3.01	3.14	0.08
	98.80	97.76	97.30	97.27	97.19	96.44	96.05	95.96	95.84	95.72	95.57	95.48	95.34	95.28	95.17	95.08	95.02	94.94	94.68	94.43	94.09	95.88		

MTR 146

	E	E	E	E	E	E	E	E	E	E	E	E	E	E	E	E	E	E	Mean	Mean norm.	σ
SiO_2	75.76	75.76	74.53	74.00	74.65	74.33	72.71	75.26	73.93	73.20	72.03	72.98	74.43	72.34	74.35	72.54	73.39	69.82	73.67	75.89	1.32
TiO_2	0.29	0.29	0.23	0.30	0.15	0.17	0.15	0.27	0.12	0.04	0.21	0.17	0.28	0.41	0.19	0.09	0.08	0.21	0.20	0.21	0.09
Al_2O_3	15.00	15.00	14.41	14.58	14.08	14.22	13.86	11.81	12.74	13.05	13.59	12.44	11.58	12.45	11.83	12.98	12.03	13.76	13.30	13.69	0.91
FeO	1.50	1.50	1.57	1.64	1.59	1.37	1.25	1.86	0.91	1.04	1.21	0.95	1.32	1.99	1.46	1.16	0.87	1.55	1.37	1.41	0.32
MnO	0.05	0.05	0.03	0.05	0.02	0.02	0.08	0.04	0.03	0.09	0.05	0.08	0.11	0.02	0.03	0.04	0.07	0.03	0.05	0.05	0.03
MgO	0.36	0.36	0.39	0.42	0.46	0.34	0.36	0.30	0.17	0.22	0.31	0.21	0.20	0.49	0.32	0.21	0.17	0.46	0.32	0.33	0.11
CaO	1.76	1.76	1.78	1.81	1.79	1.73	1.48	1.78	1.27	1.43	1.53	1.30	1.10	2.14	1.81	1.42	1.42	1.85	1.62	1.67	0.26
Na_2O	3.39	3.39	3.83	3.96	3.40	3.58	3.77	3.30	3.91	3.36	3.37	3.56	3.16	3.47	3.14	3.39	3.33	3.77	3.50	3.61	0.24
K_2O	3.15	3.15	3.17	3.06	3.09	3.09	3.27	2.18	3.60	3.52	3.24	3.64	3.07	1.88	2.05	3.33	3.50	3.05	3.06	3.15	0.53
	101.2	101.2	99.94	99.81	99.23	98.84	96.93	96.80	96.67	95.95	95.53	95.34	95.23	95.18	95.17	95.14	94.86	94.48	97.09		

Samples with a 'B' notation were analysed at Bergen; samples with an 'E' notation were analysed at Edinburgh. Full details of methodology are in the methods section.

rapid and computationally simple, although the method disregards potentially significant minor oxides, does not consider data structure, and weights all oxides equally (e.g., Payne and Blackford, 2005). The very large number of tephras that needs to be compared in a region such as Alaska makes the speed and simplicity of the SC method highly useful, although it may be best employed in combination with other techniques.

Multivariate techniques have been used to distinguish between tephras from similar sources or from the same volcanic system and are particularly useful where the major element geochemistry falls within a narrow range (Stokes and Lowe, 1988; Shane and Froggatt, 1994). In this study, the general structure of the EPMA data was investigated by indirect gradient analysis, serving here as a dimension-reduction technique to allow the multivariate data to be presented in a 2-D plot. The entire data set was analysed by principal components analysis (PCA) using log-transformed data with double centering in CANOCO ver. 4.53 (Ter Braak and Šmilauer, 1997–2004). As an additional tool to investigate the data structure and internal correlations, cluster analysis was applied (King et al., 1982). The entire data set, including all oxides, was analysed using Average-Link clustering with a squared Euclidean Distance matrix in SPSS ver. 10.

Cores were dated using radiocarbon. Material to be dated was carefully prepared using clean instruments with samples taken from the center of the cores to avoid contamination with modern carbon. Bulk samples were used for initial dates from the base of the cores, but greater precision is required for dates on tephra layers. For these samples, plant macrofossils were individually picked out, preferentially selecting *Sphagnum* leaves and stems as these are believed to be an optimal dating material (Nilsson et al., 2001). Bulk peat samples were sieved to remove fine material (<300 μm) and macrofossils were picked out under low-power microscopy at 50× magnification. Samples were carefully cleaned to remove any contaminants and washed in 10% HCl and ultrapure water. Dating was carried out at three different laboratories: a bulk sample from the Chilkoot Pond site was radiometrically dated at the Gliwice laboratory (Gd prefix); a sequence of samples across a tephra in the Point Lena site was AMS-dated at the Groningen laboratory (GrA prefix); and ten further samples were AMS-dated at the NERC radiocarbon laboratory, East Kilbride (SUERC prefix). For one tephra from the Chilkoot Pond site, a sample of *Sphagnum* leaves and a sample of *Sphagnum* stems were analysed separately to determine the impact of material choice on radiocarbon date. For the sample from 100 to 101 cm depth in the Point Lena site, two sub-samples were dated, one each at the Groningen and NERC laboratories. Radiocarbon dates were calibrated using OxCal ver. 3.10 (Bronk Ramsey, 2005). To estimate the age of tephra layers not directly dated, age–depth models were constructed using linear interpolation between dating points. Linear interpolation makes the assumptions that all radiocarbon dates are accurate and that accumulation rates change precisely at the dating point, either of which may well be misplaced. Despite these potential problems, this strategy is most appropriate when the number of dates available is limited, as in this study (Telford et al., 2004).

Results

No stratigraphically visible tephras were identified in the five cores, but optical microscopy revealed fourteen cryptotephras. A maximum of four tephras in a single site indicates that this minimum number of separate tephra fall events is recorded in the region. The stratigraphic relationships of the tephra layers have been previously described in a preliminary publication (Payne and Blackford, 2004). Tephra layers have been named by their site code and depth, so for instance the LNA 39 tephra has a peak concentration of glass shards in the sample at 39-cm depth in the Point Lena site. Glass shards were commonly small and scarce, and the available samples were comparatively small; EPMA data were only obtainable from nine of these layers (Table 1). Some analysis totals are comparatively low, probably due to shard hydration. Some analyses with low totals were excluded; however, the 95% limit advocated by Hunt and Hill (1993) was not applied to allow comparison with previous Alaskan tephra studies. Some heterogeneity in composition is apparent in some tephras (for instance MTR 146). Possible reasons for this include real magma heterogeneity (e.g., Downes, 1985; Riehle et al., in press), selective loss of volatile elements due to the use of a fixed beam, or conceivably (but unlikely) mixed tephra layers.

Correlations between tephras analysed in this study

Correlations between tephra layers in this study have been tested using oxide plots, similarity coefficients, and cluster analysis. Table 2 shows the internal SC matrix. Results show SCs greater than 0.90 between many tephra pairs and SCs greater than 0.95 between several. The SC results only provide an indication of potential correlations and data need to be interpreted with regard to the probable age and stratigraphic position of the layers. For instance, the highest SC value is 0.98 between the LNA 100 and the LNA 39 layers. These tephras occur at different depths in the same site with no evidence for disturbance of the stratigraphy. It would therefore seem extremely unlikely that these layers are correlatives. Similarly, quite high SC values are found between SPM 26 and MTR 146, LNA 39 and MTR 146, and ECR 32 and MTR 146, all of which seem improbable.

However, many of the correlations are more feasible and several distinct features are evident. The data strongly suggest

Table 2
Similarity coefficients between tephra layers in this study

Tephra	ECR 100	ECR 162	SPM 26	MTR 190	MTR 146	LNA 39	CHP 184	ECR 32	LNA 100
ECR 100	x		0.90		0.93	0.91		0.90	
ECR 162		x							
SPM 26	0.90		x		0.95	0.94	0.95	0.98	0.92
MTR 190				x			0.90		
MTR 146	0.93		0.95		x	0.96	0.95	0.96	0.95
LNA 39	0.91		0.94		0.96	x	0.93	0.96	0.98
CHP 184			0.95	0.90	0.95	0.93	x	0.97	0.92
ECR 32	0.90		0.98		0.96	0.96	0.97	x	0.94
LNA 100			0.92		0.95	0.98	0.92	0.94	x

https://doi.org/10.1016/j.yqres.2007.10.007 Published online by Cambridge University Press

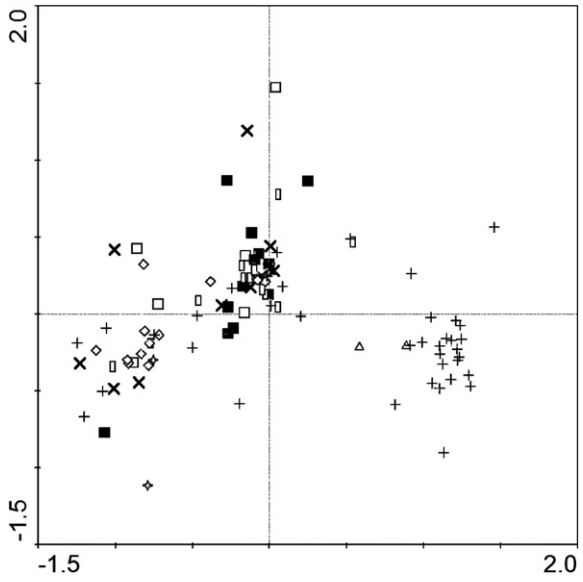

Figure 2. PCA ordination plot of EPMA data for tephra ECR 162 (crosses), ECR 100 (triangles), LNA 100 (rectangles), LNA 39 (filled squares), SPM 26 (squares), ECR 32 (Xs), MTR 190 (stars), and CHP 184 (diamonds).

correlation among SPM 26, ECR 32, and LNA 39 tephras, which have generally high SC values (>0.94) and are at similar depths. The MTR 146 tephra correlates fairly well with LNA 100 (SC=0.95) but is distinctly different in probable age and therefore probably represents a different eruption. The ECR 162 tephra is clearly the most distinct unit with limited correlations with all the other tephras (SCs <0.90). Analyses of only two shards were obtained on the MTR 190 and ECR 100 tephras but these also appear to be distinct units.

The results of the PCA are shown in Figure 2. All tephras show considerable scatter, the most distinct feature being the separation of the ECR 162 analyses from the rest. The CHP 184 analyses are clustered to the left of the plot but overlap with some of the other data points. Table 3 shows groups assigned by cluster analysis at the second level from the top (arbitrarily chosen).

Cluster analysis of the data set highlights four groups. Group one is the largest and includes the majority of the data: all analyses from SPM 26, CHP 184, and ECR 32 tephras; the majority of analyses of glass from LNA 39, LNA 100, and MTR 146 tephras; and one analysis from MTR 190 tephra. Group 2 includes all ECR 162 analyses and no other. Group 3 includes two analyses of LNA 100 tephra and one of LNA 39; these analyses are differentiated by low sodium contents and may be best considered as analyses in which distinct sodium mobilisation occurred (Froggatt, 1983; Hunt and Hill, 1993). Group 4 includes three analyses of MTR 146, both analyses of ECR 100, and one analysis of MTR 190 tephra, differentiated by high SiO_2 and/or low K_2O.

Taken overall, the data analyses suggest several features of the data:

1. The ECR 162 tephra is clearly the most distinct unit with low similarity coefficients with the other tephras and all analyses forming a distinct group in the cluster analysis.
2. The ECR 100 is probably also a distinct layer (although only two analyses were obtained).
3. Similarly, only two analyses were obtained from the MTR 190. These analyses are different from each other and are assigned to different cluster analysis groups; however, both of these analyses are quite distinct and suggest that this tephra is probably a distinct unit.
4. There is broad similarity in glass composition among CHP 184, MTR 146, LNA 100, SPM 26, ECR 32, and LNA 39 tephras. Stratigraphic position strongly suggests correlation among SPM 26, ECR 32, and LNA 39 tephras (although inferred ages vary). The MTR 146 and LNA 100 tephras are probably separate units.
5. The correlation of the CHP 184 tephra is uncertain. It may have the same source as one of the other units, but it may be from a different eruption.

These overall groupings are used to compare these tephras to data from other Alaskan studies. The tephra layers without EPMA data cannot be reliably correlated. However, similarity in depth suggests that the CHP 33 and the MTR 32 tephras may well correlate with the LNA 39, the SPM 26, and the ECR 32 group.

Correlations with data from previous studies

The internal comparisons suggest correlation among ECR 32, LNA 39, and SPM 26 layers. All of these tephras show strong similarity to the White River Ash (WRA). SCs are as great as 0.99 with proximal WRA deposits and 0.96 with distal

Table 3
Cluster analysis results

Group	Members
Group 1	SPM 26 (6 analyses), LNA 39 (11 analyses), CHP 184 (12 analyses), LNA 100 (10 analyses), MTR 146 (15 analyses), ECR 32 (12 analyses), MTR 190 (1 analysis)
Group 2	ECR 162 (21 analyses)
Group 3	LNA 100 (2 analyses), LNA 39 (1 analysis)
Group 4	MTR 146 (3 analyses), ECR 100 (2 analyses), MTR 190 (1 analysis)

Table 4
Similarity coefficients of Southeast Alaska tephra with selected previous analyses of WRA tephra

	Proximal WRA (Richter et al., 1995; 90Adg-2 and WR91-1)		Distal WRA (Downes, 1985; 69–65, 69–69, 87–89a, and 87–89b)			
SPM 26	0.97	0.95		0.96	0.94	0.94
LNA 39	0.96	0.97	0.95	0.94	0.96	0.95
ECR 32	0.99	0.97	0.92	0.95	0.94	0.94
LNA 100	0.95	0.96	0.96	0.93	0.95	0.95
MTR 146	0.97	0.96	0.92	0.95	0.92	0.94
CHP 184	0.95	0.93		0.93	0.90	0.90

https://doi.org/10.1016/j.yqres.2007.10.007 Published online by Cambridge University Press

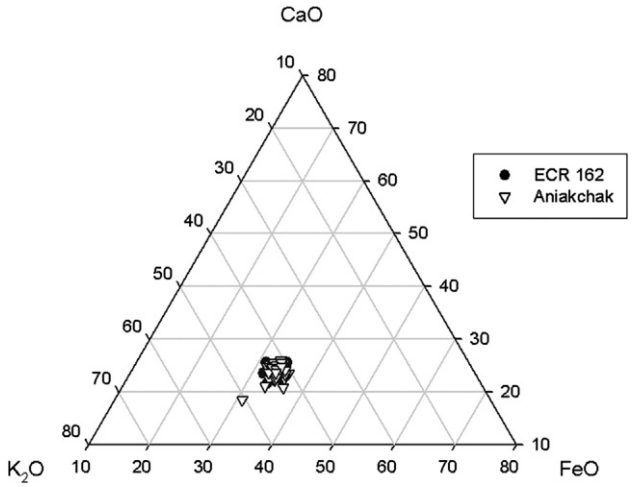

Figure 3. Ternary plot showing relative percentages of three major oxides for selected tephra layers in this study and White River Ash reference data (Begét et al., 1992; Downes, 1985; Richter et al., 1995).

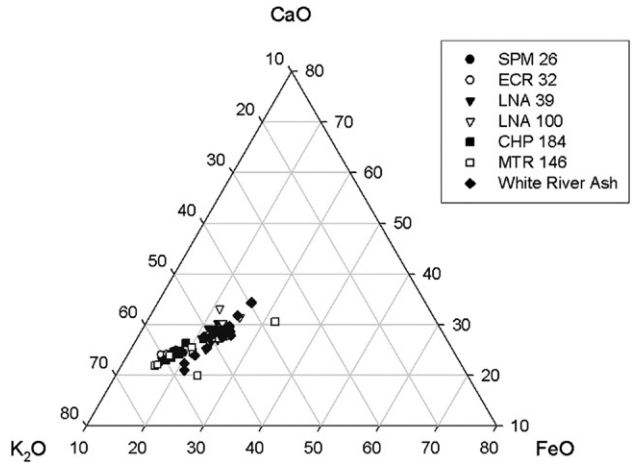

Figure 4. Ternary plot showing relative percentages of three major oxides for ECR 162 tephra and Aniakchak tephra in Western Alaska (Payne, 2005; sites AKH and ESP).

deposits (Table 4). Most SCs exceed the usual 0.95 criterion for correlation.

There is also similarity in the composition of CHP 184, MTR 146, and LNA 100 tephras, although considerable differences in their probable age. Similarity coefficients of these tephras with WRA reference data are also high; SCs exceed 0.95 with at least one of the established data sets (Table 4). Similarity coefficients are most convincing with the LNA 100 tephra, with five of the values exceeding 0.95, and least convincing with the CHP 184 tephra, with only one of the SCs exceeding 0.95. A ternary diagram comparing CHP 184, MTR 146, LNA 100, SPM 26, LNA 39, and ECR 32 with the White River Ash reference data shows a convincing overlap (Fig. 3), providing evidence that these tephras are the WRA or have the same source. By contrast, SCs with many other tephras compared do not exceed 0.95. There is no significant difference in correlation to the Northern or Eastern lobe WRA data presented by Downes (1985).

Analyses of ECR 100, MTR 190, and ECR 162 tephras show only limited agreement with those of other tephras in this study and are likely to be distinct units. The ECR 100 data are from only two shards, making definitive correlation difficult. These shards show the greatest similarity to proximal tephra from Augustine Volcano (Riehle, 1985), although SCs do not exceed the 0.95 criterion (SCs $\leq$0.94; Table 5). Due to the limited data and the imperfect correlation, the tephra cannot be firmly attributed, but Augustine Volcano is provisionally suggested as the source. The MTR 190 data are also from only two analyses and these shards are different from each other. The averaged composition shows a high degree of similarity to distal tephra from Mt. Redoubt. Similarity coefficients with ca. 350, ca. 400, and 500+ cal yr BP tephras on the Kenai Peninsula are >0.96 with at least one data set each (Begét et al., 1994; Table 5). These correlations provide evidence for a Redoubt origin, although the limited size of the data set and difference between the shards means that this must be treated with caution.

The ECR 162 tephra is the most clearly distinct identified tephra. Similarity coefficients with Aniakchak tephra in western Alaska are high ($\geq$0.95); by contrast, SCs with other tephras in the comparison set do not exceed 0.92. Major element ranges overlap with the Aniakchak data in a ternary plot (Fig. 4), providing further support for correlation.

Dating the tephras

In all five of these studied sites, a tephra layer is present in the uppermost 40 cm of peat. EPMA data from tephra from three of these sites (SPM 26, LNA 39, and ECR 32) strongly suggest correlation. Although the MTR 32 and CHP 33 tephras do not

Table 5
Similarity coefficients of southeast Alaska with selected analyses of other Alaskan tephras

	Augustine (Riehle, 1985; RBW75A and RBW33D)		Aniakchak (R. Payne, unpublished data; AKH 44 and ESP 38)		Redoubt 1989/1990 (Begét et al., 1994; ACT 66 and 4/8/90)		Redoubt ca. 350 cal yr BP (Begét et al., 1994; SK-11-2-12 and SK-10-2-20)		Redoubt ca. 400 cal yr BP (Begét et al., 1994; SK-11-3-15 and SK-10-2-2-5)		Redoubt ca. 500 cal yr BP (Begét et al., 1994; SK-6-1-42)
ECR 100	0.94	0.94									
ECR 162			0.95	0.96							
MTR 190					0.93	0.93	0.95	0.96	0.95	0.96	0.96

https://doi.org/10.1016/j.yqres.2007.10.007 Published online by Cambridge University Press

Table 6
Radiocarbon dating evidence from the five peat cores

Site	Depth (cm)	Laboratory code	Technique	Material	Adjacent tephra (if any)	Uncalibrated age (^{14}C yr BP)	Calibrated age range (cal yr BP, 95% probability)
Chilkoot Pond	33–34	SUERC-5914	AMS	*Sphagnum* leaves	CHP 33	257±22	280–320
	33–34	SUERC-5919	AMS	*Sphagnum* stems	CHP 33	299±24	460–290
	140–152	Gd-15809	Radiometric	Bulk peat		470±80	310–570
	175–176	SUERC-565	AMS	Bulk peat		468±55	410–570
Mount Riley	210–211	SUERC-564	AMS	Bulk peat		8688±65	9530–9890
Spaulding Meadows	196–197	SUERC-566	AMS	Bulk peat		7207±53	7940–8170
Eaglecrest	162–163	SUERC-5917	AMS	*Sphagnum* leaves	ECR 162	4485±30	5030–5300
	195–196	SUERC-567	AMS	Bulk peat		6183±56	6940–7250
	365–366	SUERC-568	AMS	Bulk peat		9244±49	10260–10560
Point Lena	97–98	GrA-28701	AMS	*Sphagnum* leaves	Bounding LNA 100	1415±35	1285–1380
	98–99	GrA-28709	AMS	*Sphagnum* leaves	Bounding LNA 100	1565±35	1380–1540
	99–100	GrA-28707	AMS	*Sphagnum* leaves	Bounding LNA 100	1630±35	1410–1610
	100–101	GrA-28706	AMS	*Sphagnum* leaves	LNA 100	1380±35	1260–1360
	100–101	SUERC-5913	AMS	*Sphagnum* leaves	LNA 100	1428±28	1290–1375
	101–102	GrA-28705	AMS	*Sphagnum* leaves	Bounding LNA 100	1460±35	1300–1410
	102–103	GrA-28703	AMS	*Sphagnum* leaves	Bounding LNA 100	1365±35	1180–1350
	103–104	GrA-28702	AMS	*Sphagnum* leaves	Bounding LNA 100	1455±35	1290–1400
	275–276	SUERC-569	AMS	Bulk peat		2423±51	2340–2620
	520–521	SUERC-570	AMS	Bulk peat		7919±83	8580–9010

have geochemical data, the similarity in depth suggests that they are correlatives. The CHP 33 tephra has been directly radiocarbon dated. A sample of *Sphagnum* leaves gave an age estimate of 280–320 cal yr BP (Table 6) and a sample of *Sphagnum* stems gave a marginally less precise date with a calibrated age range of 290–460 cal yr BP, supporting the choice of *Sphagnum* leaves for the other dates. The CHP 33 tephra was therefore deposited around 300 cal yr BP. Although the CHP 33 tephra does not have EPMA data, the balance of probability suggests that a single tephra layer was deposited at all five sites around 300 cal yr BP, or approximately AD 1650.

A sequence of dates were obtained on the LNA 100 tephra with the intention of wiggle-matching the tephra age (Blaauw et al., 2004). An initial date on the glass shard peak (100–101 cm; SUERC-5913) gave a calibrated age range of 1290–1375 cal yr BP. A sequence of dates from 97 to 104 cm give an overall calibrated age span of 1180–1610 cal yr BP. There is considerable variability in these dates and they do not form a coherent stratigraphic sequence (Table 6). The variability in the dates does not correspond to wiggles in the calibration curve, making wiggle-matching impossible. Reasons for the unexpected sequence of dates are uncertain. Two independent dates have been obtained on the horizon containing the cryptotephra at 100–101 cm (Table 6). These produced overlapping calibrated age ranges of 1260–1360 and 1290–1375 cal yr BP, providing a consistent age estimate for the LNA 100 tephra.

The ECR 162 tephra has been dated to 5030–5300 cal yr BP (SUERC-5917; Table 6). ECR 100, MTR 146, and MTR 190 tephras were not directly dated. Age–depth interpolation suggests that the ECR 100 tephra was deposited ca. 2840 cal yr BP, the MTR 146 tephra ca. 6300 cal yr BP, and the MTR 190 tephra ca. 8660 cal yr BP.

Discussion

Source of the tephras

All of the sites contain a tephra layer dating to ca. 300 cal yr BP (AD 1650) with a major element geochemistry similar to that of the White River Ash. Both the eastern and northern lobe WRA deposits are considerably older, around 1147 and 1890 cal yr BP, respectively (Lerbekmo et al., 1975; Clague et al., 1995). Accumulation rates of ombrotrophic mires are usually in the range 10–20 yr cm^{-1}. Robinson and Moore (1999) reported the depth of the WRA tephra in western Canadian peatlands; in ombrotrophic sites, the mean depth of the tephra was 68 cm whereas in poor fens it was 54 cm. The sites in this study are farther south in a more climatically favourable location for peat accumulation. It is therefore extremely unlikely that a tephra at this depth could be a correlative of either of the WRA deposits. No younger eruptions are known from Mt. Churchill. The only volcano in the Wrangell Volcanic Field to have had historic-age eruptions is Mt. Wrangell. However, there are no known eruptions near the probable age of this tephra, and the high degree of geochemical similarity to the WRA means a different source is improbable. The most likely source of the tephras is therefore a previously unknown eruption of Mt. Churchill, within the last 600 yr, and most probably around AD 1650. We propose the name ‘Lena tephra’ for this layer following the convention of naming previously unknown tephras after the site in which they were first located.

MTR 146, LNA 100, and CHP 184 tephras also bear geochemical similarity to the WRA. The MTR 146 tephra is dated at ca. 6330 cal yr BP. While this estimate is based on extrapolation and must be treated with caution, the sequence appears to be complete and to span most of the Holocene so this

https://doi.org/10.1016/j.yqres.2007.10.007 Published online by Cambridge University Press

tephra is almost certainly mid-Holocene in age. It is therefore unlikely to be either of the WRA eruptions. The most probable source is another previously unidentified eruption of Mt. Churchill.

The age of the CHP 184 tephra is uncertain. Peat accumulation at this site appears to have undergone an unusual pattern as this depth of peat would usually represent several thousand years. The closest dates to the tephra here are around 500 cal yr BP. Given this level of uncertainty, the layer may be the Lena tephra but could also be the WRA tephra, the mid-Holocene tephra identified at MTR 146, or even yet another similar tephra.

The LNA 100 tephra shows geochemical similarity to WRA tephra. Dating evidence does not show a consistent sequence of radiocarbon dates but samples from peat containing the ash layer suggest that the tephra was deposited between approximately 1260 and 1375 cal yr BP. The most likely origin of this tephra is therefore one of the WRA eruptions, most probably the younger, eastern lobe event. Clague et al. (1995) presented ten radiocarbon assays on this tephra spanning 791 to 1416 cal yr BP and opted for a weighted mean of four of these dates to assign the eruption an age estimate of ca. 1147 cal yr BP. The dates in this study would suggest an older date for this tephra, although this conclusion is complicated by the dates being out of sequence (Table 6).

The ECR 162 tephra is the most geochemically distinctive tephra located in these sites. EPMA data suggest a good correlation with tephra from Aniakchak. The tephra is dated 5300–5030 cal yr BP, considerably older than the very large caldera-forming event in the fourth millennium BP (Aniakchak II; Miller and Smith, 1987; Begét et al., 1992). A previous caldera-forming event is probably older than this tephra (ca. 8200 cal yr BP; VanderHoek and Myron, 2004). There are no known Aniakchak eruptions around this date. Miller and Smith (1987) discussed an eruption of the adjacent Black Peak with an uncalibrated date of 4470 ± 200 ^{14}C yr BP, very close to the uncalibrated date of ECR 162 at 4485 ± 30 ^{14}C yr BP. However, geochemical similarity with Black Peak tephra is low, although there are comparatively few published data from this volcano (Riehle et al., 1999). Despite the similarity in age with Black Peak, based on the geochemical composition the most probable source of the tephra is a previously unknown eruption of Aniakchak.

The ECR 100 tephra shows greatest similarity to tephra from Augustine Volcano, although correlations are imperfect and the data set very small. The age–depth model places the tephra at ca. 2840 cal yr BP. Little is known about the distribution of tephra from Augustine eruptions prior to ca. AD 200 (Begét and Kienle, 1992; Waitt and Begét, in press). The source of the tephra cannot be reliably determined, although an Augustine eruption is tentatively suggested as the most likely based on available evidence. Limited data for the MTR 190 tephra show some similarity to tephras from Redoubt Volcano. The age–depth model places the layer at ca. 8660 cal yr BP; the closest Redoubt eruption to this date has an uncorrected radiocarbon date of 7730 ± 150 ^{14}C yr BP (7050–6250 cal yr BP). This eruption may be the most likely candidate for the source of this tephra but uncertainties remain.

Implications for Alaskan tephrochronology

Results of this study reveal the presence of several Holocene cryptotephra layers in southeast Alaskan peatlands. The tephras originated from eruptions of Mt. Churchill, Aniakchak, and possibly Augustine and Redoubt volcanoes. Ages assigned to these tephras by radiocarbon dating and age–depth models provide new regional iochrons. In several cases, the cryptotephras appear to be from previously unknown eruptions. Perhaps the most interesting find is the widespread Lena tephra at ca. 300 cal yr BP. This tephra was found in all five study sites and may prove to be a very useful late Holocene isochron. The western European cryptotephra record has shown that cryptotephra layers can be formed at great distance even from comparatively minor eruptions (Dugmore et al., 1996). Therefore, the eruptions that formed the cryptotephras identified here were not necessarily particularly large, and this might explain why they have apparently been overlooked in proximal studies.

None of the tephras identified appear to be from Mt. Edgecumbe, the only volcano in the southeast Alaskan panhandle. Similarity coefficients with geochemical data from the Younger Dryas-age Edgecumbe tephra are low ($SC < 0.85$). Although there are no comparative data from the mid-Holocene eruptions, the geochemical composition would most probably be expected to be broadly similar. These results therefore suggest that the mid-Holocene eruptions were either very minor, or that unlike the Younger Dryas eruption, tephra plumes were not directed north towards these sites.

An important issue with distal tephrochronology in Alaska, and particularly with cryptotephrochronology, is the current lack of comparative data. Eruption frequencies suggest that Alaskan volcanoes have produced many thousands of Holocene tephra layers. However, the limited tephra research in Alaska means that only a small minority of these tephras have geochemical data or age estimates. It is therefore difficult to make correlations and to identify a probable source when trying to identify unknown distal tephras that may be from relatively minor eruptions. The tephra identifications reported here could require revision as more data sets become available. More tephrochronological research, including cryptotephra studies, is required throughout Alaska.

Our findings demonstrate that microscopic methods can reveal the presence of Holocene tephra layers in regions for which none were previously known. Results provide an outline Holocene cryptotephrochronology for southeast Alaska that will aid dating of palaeoenvironmental records. Future studies may improve age estimates and may identify further tephras to extend this scheme. Using these methods, it seems probable that tephrochronology could be used much more widely than has been recognized so far. If cryptotephras can be found in these sites (and from volcanoes as distant as Aniakchak), it seems probable that such cryptotephras could also be found through most of sub-Arctic Alaska.

Implications for volcano hazard assessment

Results of this study suggest that Mt. Churchill, source of the White River Ash, has had more Holocene activity than

https://doi.org/10.1016/j.yqres.2007.10.007 Published online by Cambridge University Press

previously recognized. Previously, only two Holocene eruptions were recognized from Mt. Churchill, forming the northern and eastern White River Ash deposits. The Lena tephra appears to represent a Mt. Churchill eruption approximately 300–350 yr ago and the MTR 146 tephra may record a further mid-Holocene eruption, suggesting at least four Holocene eruptions have occurred. There is evidence that the WRA eruptions may have had significant impacts on human occupation of the region (Workman, 1979; Moodie et al., 1992). It is possible that these previously unidentified eruptions may also have had significant impacts on the physical and human environment of the region. The region of eastern Alaska and western Canada surrounding the volcano is sparsely populated compared to many areas of North America. However, given the intensity and the extent of tephra deposition from previous eruptions, the hazard risk is not insignificant. The results here suggest that the eruptive history of Mt. Churchill may have been underestimated; there may therefore be a case for re-assessing the hazard posed by the volcano.

Conclusions

This study demonstrates the presence of Holocene cryptotephras in the peatlands of southeast Alaska. Cryptotephrochronology may be usefully applied in many regions of the world beyond the scope of conventional tephrochronology, allowing dating of sediments and an improved understanding of volcanic history (e.g., Gehrels et al., 2006). Results here highlight the eruptive history of Mt. Churchill. The Wrangell Volcanic Field has generally received less attention from volcanologists and tephrochronologists than the volcanoes of the Aleutian Arc. This is perhaps understandable given the greater number of volcanoes in southwest Alaska, combined with the more densely populated regions of the Kenai Peninsula and Anchorage Bowl and the presence of international air routes. However, the Wrangell Volcanic Field is the source of two of the largest North American eruptions in the last two thousand years, and the risk posed by an eruption of this scale is considerable. More tephra studies will help our understanding of the long-term volcanic history of the region; cryptotephrochronology should play an important role in this research.

Acknowledgments

RJP's work was supported by a QMUL Westfield studentship and an EU Marie Curie training site fellowship. Microprobe time at Edinburgh was funded by the Natural Environment Research Council and at Bergen by the EU. Thanks to Peter Hill, Anthony Newton, Haflidi Haflidason, and Ole Tumyr for microprobe assistance. Fieldwork funding was provided by The Royal Society, the University of London Central Research Fund, the Dudley Stamp Memorial Fund, and the Quaternary Research Association. SUERC dates were funded by the Natural Environment Research Council (Allocation no. 1101.1004). We are grateful to Cathy Connor (University of Alaska, South East), Kristi Wallace, and Tina Neal (USGS) for discussion of field sites and Alaskan tephras. Thanks to David Lowe and Jim Begét for helpful reviews of a previous version of the manuscript.

References

Aaby, B., Digerfeldt, G., 1986. Sampling techniques for lakes and bogs, In: Berglund, B. (Ed.), Handbook of Holocene palaeoecology and palaeohydrology. Wiley, Chichester.

Begét, J., Kienle, J., 1992. Cyclic formation of debris avalanches at Mount St Augustine volcano. Nature 356, 701–704.

Begét, J., Motyka, R., 1998. New dates of late Pleistocene dacitic tephra from the Mount Edgecumbe Volcanic field, Southeastern Alaska. Quaternary Research 49, 123–125.

Begét, J., Reger, R., Pinney, D., Gillispie, T., Campbell, K., 1991. Correlation of the Holocene Jarvis Creek, Tangle Lakes, Cantwell and Hayes tephras in south-central and central Alaska. Quaternary Research 35, 174–189.

Begét, J., Mason, O., Anderson, P., 1992. Age, extent and climatic significance of the c. 3400 BP Aniakchak tephra, Western Alaska, USA. The Holocene 2, 51–56.

Begét, J.E., Stihler, S.D., Stone, D.B., 1994. A 500-year-long record of tephra falls from Redoubt volcano and other volcanoes in upper Cook Inlet, Alaska. Journal of Volcanology and Geothermal Research 62, 55–67.

Bergman, J., Wastegård, S., Hammarlund, D., Wohlfarth, B., Roberts, S.J., 2004. Holocene tephra horizons at Klocka Bog, west-central Sweden: Aspects of reproducibility in subarctic peat deposits. Journal of Quaternary Science 19, 241–249.

Birks, H.H., Gulliksen, S., Haflidason, H., Mangerud, J., Possnert, G., 1996. New radiocarbon dates for the Vedde ash and the Saksunavtn ash from western Norway. Quaternary Research 45, 119–127.

Blackford, J., Edwards, K., Dugmore, A., Cook, G., Buckland, P., 1992. Icelandic volcanic ash and mid-Holocene Scots pine (*Pinus sylvestris*) pollen decline in northern Scotland. The Holocene 2, 260–265.

Blaauw, M., van Geel, B., Mauquoy, D., van der Plicht, J., 2004. Carbon-14 wiggle-match dating of peat deposits: Advantages and limitations. Journal of Quaternary Science 19, 177–181.

Blockley, S.P.E., Pyne-O'Donell, S.D.F., Lowe, J.J., Pollard, A.M., Matthews, I.P., Molyneux, E.G., Turney, C.S.M., 2005. A new & less destructive laboratory procedure for the physical separation of distal glass tephra shards from sediments. Quaternary Science Reviews 24, 1952–1960.

Borchardt, G.A., Aruscavage, P.J., Miller, H.T., 1972. Correlation of the Bishop ash, a Pleistocene marker bed, using instrumental neutron activation analysis. Journal of Sedimentary Petrology 42, 301–306.

Bronk Ramsey, C., 2005. OxCal program v.3.10. Oxford University.

Buckley, S., Walker, M.J.C., 2002. A mid-Flandrian tephra horizon, Cambrian Mountains, west Wales. Quaternary Newsletter 96, 5–11.

Caseldine, C.J., Hatton, J.M., Huber, U.M., Chiverrell, R., Woolley, N., 1998. Assessing the impact of volcanic activity on mid-Holocene climate in Ireland: The need for replicate data. The Holocene 8, 105–111.

Chambers, F.M., Daniell, J.R.G., Hunt, J.B., Molloy, K., O 'Connell, M., 2004. Tephrostratigraphy of An Loch Mor, Inis Oirr, western Ireland: Implications for Holocene tephrochronology in the northeastern Atlantic region. The Holocene 14, 703–720.

Child, J., Begét, J., Werner, A., 1998. Three Holocene tephras identified in Lacustrine sediment cores from the Wonder Lake area, Denali National Park and Preserve, Alaska USA. Arctic and Alpine Research 30, 89–95.

Clague, J.J., Evans, S.G., Rampton, V.N., Woodsworth, G.J., 1995. Improved age estimates for the White River and Bridge River tephras, western Canada. Canadian Journal of Earth Sciences 32, 1172–1179.

Dachnowski-Stokes, A., 1941. Peat resources in Alaska. US Department of Agriculture Technical Bulletin 769, 1–84.

Davies, S.M., Hoek, W.Z., Bohncke, S.J.P., Lowe, J.J., Pyne O'Donnell, S., Turney, C.S.M., 2005. Detection of late-glacial distal tephra layers in the Netherlands. Boreas 34, 123–135.

Downes, H., 1985. Evidence for magma heterogeneity in the White River Ash (Yukon Territory). Canadian Journal of Earth Sciences 22, 929–934.

Dugmore, A., 1989. Icelandic volcanic ash in Scotland. Scottish Geographical Magazine 105, 168–172.

Dugmore, A., Newton, A., 1992. Thin tephra layers in peat revealed by X-radiography. Journal of Archaeological Science 19, 163–170.

Dugmore, A., Larsen, G., Newton, A., Sugden, D., 1992. Geochemical stability of fine-grained silicic Holocene tephra in Iceland and Scotland. Journal of Quaternary Science 7, 173–183.
Dugmore, A., Larsen, G., Newton, A., 1995. Seven tephra isochrones in Scotland. The Holocene 5, 257–266.
Dugmore, A.J., Newton, A.J., Edwards, K.J., Larsen, G., Blackford, J.J., Cook, G.T., 1996. Long-distance marker horizons from small-scale eruptions: British tephra deposits from the AD 1510 eruption of Hekla, Iceland. Journal of Quaternary Science 11, 511–516.
Dwyer, R.B., Mitchell, F.J.G., 1997. Investigation of the environmental impact of remote volcanic activity on north Mayo, Ireland, during the mid-Holocene. The Holocene 7, 113–118.
Froggatt, P.C., 1983. Toward a comprehensive upper Quaternary tephra and ignimbrite stratigraphy in New Zealand using electron microprobe analysis of glass shards. Quaternary Research 19, 188–200.
Gehrels, M.J., Lowe, D.J., Hazell, Z.J., Newnham, R.M., 2006. A continuous 5300-yr Holocene cryptotephrostratigraphic record from northern New Zealand and implications for tephrochronology and volcanic hazard assessment. The Holocene 16, 173–187.
Gronvold, K., Oskarsson, N., Johnsen, S.J., Clausen, H.B., Hammer, C.U., Bond, G., Bard, E., 1995. Ash layers from Iceland in the Greenland GRIP ice core correlated with oceanic and land based sediments. Earth and Planetary Science Letters 54, 238–246.
Hodder, A.P.W., De Lange, P.J., Lowe, D.J., 1991. Dissolution and depletion of ferromagnesian minerals from Holocene tephra layers in an acid bog, New Zeland, and implications for tephra correlation. Journal of Quaternary Science 6, 195–208.
Hunt, J., Hill, P., 1993. Tephra geochemistry: a discussion of some persistent analytical problems. The Holocene 3, 271–278.
King, R.H., Kingston, M.S., Barnett, R.L., 1982. A numerical approach to the classification of magnetites from tephra in southern Alberta. Canadian Journal of Earth Sciences 19, 2012–2019.
Lerbekmo, J.F., Campbell, F.A., 1969. Distribution, composition and source of the White River Ash, Yukon Territory. Canadian Journal of Earth Sciences 6, 109–116.
Lerbekmo, J.F., Westgate, J.A., Smith, D.G.W., Denton, G.H., 1975. New data on the character and history of the White River volcanic eruption, Alaska. Quaternary studies: Selected papers from IX INQUA congress. Royal Society of New Zealand Bulletin, vol. 13, pp. 203–209.
Lowe, D.J., Hunt, J.B., 2001. A summary of terminology used in tephra-related studies. In: Juvigné, E., Raynal, J-P. (Eds.), Tephra: Chronology, Archaeology. Les Dossiers de l'Archéo-Logis, vol. 1, pp. 17–22.
Mangerud, J., Lie, S.E., Furnes, H., Kristiansen, I.L., Lomo, L., 1984. A Younger Dryas ash bed in western Norway and its possible correlations with tephra in cores from the Norwegian Sea and the North Atlantic. Quaternary Research 21, 85–104.
McKenzie, G., 1970. Some properties and age of volcanic ash in Glacier Bay National Monument. Arctic 23, 46–49.
Merkt, J., Muller, H., Knabe, W., Muller, P., Weiser, T., 1993. The early Holocene Saksunarvatn Tephra found in lake sediments in N.W. Germany. Boreas 22, 93–100.
Miller, T., Smith, R., 1987. Late Quaternary caldera-forming eruptions in the eastern Aleutian volcanic arc, Alaska. Geology 15, 434–438.
Moodie, D.W., Catchpole, A.J.W., Abel, K., 1992. Northern Athapaskan oral traditions and the White River volcano. Ethnohistory 39, 148–171.
Nilsson, M., Klarqvist, M., Bohlin, E., Possnert, G., 2001. Variation in 14C age of macrofossils and different fractions of minute peat samples dated by AMS. The Holocene 11, 579–586.
Payne, R., Blackford, J., 2004. Distal tephra deposits in southeast Alaskan peatlands. In: Emond, D., Lewis, L. (Eds.), Yukon Exploration and Geology 2003. Yukon Geological Survey, Whitehorse, pp. 191–197.
Payne, R., Blackford, J., 2005. Microwave digestion and the geochemical stability of tephra. Quaternary Newsletter 106, 24–33.
Payne, R., Kilfeather, A., van der Meer, J., Blackford, J., 2005. Experiments on the taphonomy of tephra in peatlands. Suo 56, 147–156.
Persson, C., 1971. Tephrochronological investigations of peat deposits in Scandinavia and on the Faroe Islands. Sveriges Geologiska Undersokning 65, 3–34.
Pilcher, J., Hall, V., 1992. Towards a tephrochronology for the Holocene of the north of Ireland. The Holocene 2, 255–259.
Pilcher, J., Hall, V., McCormac, F., 1995. Dates of Holocene Icelandic volcanic eruptions from tephra layers in Irish peats. The Holocene 5, 103–110.
Pilcher, J.R., Hall, V.A., 1996. A tephrochronology for the Holocene of the north of England. The Holocene 6, 100–105.
Pollard, A.M., Blockley, S.P.E., Ward, K.R., 2003. Chemical alteration of tephra in the depositional environment: theoretical stability modeling. Journal of Quaternary Science 18, 385–394.
Richter, D.H., Preece, S.J., McGimsey, R.G., Westgate, J.A., 1995. Mount Churchill, Alaska: Source of the late Holocene White River Ash. Canadian Journal of Earth Sciences 32, 741–748.
Riehle, J.R., 1985. A reconnaissance of the major Holocene tephra deposits in the upper Cook Inlet, Alaska. Journal of Volcanology and Geothermal Research 26, 37–54.
Riehle, J.R., 1996. Mount Edgecumbe volcanic field: A geologic history. U.S. Forest Service, Juneau, Alaska.
Riehle, J.R., Brew, D.A., 1984. Explosive latest Pleistocene(?) and Holocene activity of the Mount Edgecumbe Volcanic Field, Alaska. U.S. Geological Survey Circular 939, 111–114.
Riehle, J., Bowers, P., 1990. The Hayes tephra deposits, an upper Holocene marker horizon in south-central Alaska. Quaternary Research 33, 276–290.
Riehle, J., Meyer, C., Ager, T., Kaufmann, D., Ackerman, R., 1987. The Aniakchak tephra deposit, a late Holocene marker horizon in Western Alaska. U.S. Geological Survey Circular 998, 19–22.
Riehle, J.R., Mann, D.H., Peteet, D.M., Engstrom, D.R., Brew, D.A., Meyer, C.E., 1992. The Mount Edgecumbe tephra deposits, a marker horizon in southeastern Alaska near the Pleistocene–Holocene boundary. Quaternary Research 37, 183–202.
Riehle, J.R., Meyer, C.E., Miyaoka, R., 1999. Data on Holocene tephra (volcanic ash) deposits in the Alaska peninsula and lower Cook Inlet region of the Aleutian volcanic arc, Alaska. U.S. Geological Survey Open-File 99–135.
Riehle, J.R., Ager, T.A., Reger, R.D., Pinney, D.S., Kaufman, D.S., in press. Stratigraphic and compositional complexities of the late Quaternary Lethe tephra in south-central Alaska. Quaternary International. doi:10.1016/j.quaint.2006.09.006.
Rigg, G., 1914. Notes on the flora of some Alaskan *Sphagnum* bogs. The Plant World 17, 167–182.
Rigg, G., 1937. Some raised bogs of Southeastern Alaska with notes on flat bogs and muskegs. American Journal of Botany 24, 194–198.
Robinson, S.D., 2001. Extending the late Holocene White River Ash distribution, northwestern Canada. Arctic 54, 157–161.
Robinson, S.D., Moore, T.R., 1999. Carbon and peat accumulation over the past 1200 years in a landscape with discontinuous permafrost, northwestern Canada. Global Biogeochemical cycles 13, 591–601.
Rose, N., Golding, P., Battarbee, R., 1996. Selective concentration and enumeration of tephra shards from lake sediment cores. The Holocene 6, 243–246.
Shane, P.A.R., Froggatt, P.C., 1994. Discriminant function analysis of New Zealand and North American tephra deposits. Quaternary Research 41, 70–81.
Stockmarr, J., 1971. Tablets with Spores used in Absolute Pollen Analysis. Pollen et Spores 13, 615–621.
Stokes, S., Lowe, D.J., 1988. Discriminant function analysis of late Quaternary tephras from five volcanoes in New Zealand using glass shard major element chemistry. Quaternary Research 30, 270–283.
Telford, R.J., Heegaard, E., Birks, H.J.B., 2004. All age–depth models are wrong: But how badly? Quaternary Science Reviews 23, 1–5.
Ter Braak, C., Šmilauer, P., 1997–2004. CANOCO for Windows, Version 4.53, Biometris-Plant Research, Wageningen, The Netherlands.
Van den Bogaard, C., Schmincke, H.-U., 2002. Linking the North Atlantic to central Europe: A high-resolution tephrochronological record from northern Germany. Journal of Quaternary Science 17, 3–20.
VanderHoek, R., Myron, R., 2004. Cultural Remains from a Catastrophic Landscape: An Archeological Overview and Assessment of Aniakchak National Monument and Preserve. United States Department of the Interior, National Park Service, Aniakchak National Monument and Preserve.

van den Bogaard, C., Schmincke, H.-U., 2002. Linking the North Atlantic to central Europe: a high resolution Holocene tephrochronological record from northern Germany. Journal of Quaternary Science 17, 3–20.

Waitt, R., Begét, J., in press. Geologic mapping at Augustine Volcano, Alaska. USGS Professional Paper.

Wastegård, S., Björck, S., Grauert, M., Hannon, G.E., 2001. The Mjáuvøtn tephra and other Holocene tephra horizons from the Faroe Islands: a link between the Icelandic source region, the Nordic Seas, and the European continent. The Holocene 11, 101–109.

Workman, W.B., 1979. The significance of volcanism in the prehistory of subarctic northwest North America. In: Sheets, P., Grayson, D.K. (Eds.) Volcanic Activity and Human Ecology. Academic Press, New York, pp. 339-371.

Zoltai, S., 1988. Late Quaternary volcanic ash in the peatlands of central Alberta. Canadian Journal of Earth Science 26, 207–214.